

# The Use of Transit Timing to Detect Extrasolar Planets with Masses as Small as Earth

Matthew J. Holman,<sup>1\*</sup> Norman W. Murray<sup>2,3</sup>

<sup>1</sup>Harvard-Smithsonian Center for Astrophysics,  
MS51, 60 Garden Street, Cambridge, MA 02138, USA

<sup>2</sup>Canadian Institute for Theoretical Astrophysics, University of Toronto,  
60 St. George Street, Toronto, ON M5S 3H8, Canada

<sup>3</sup>Canada Research Chair

\*To whom correspondence should be addressed; E-mail: mholman@cfa.harvard.edu.

Submitted to *Science*, 17 November 2004.

**Future surveys for transiting extrasolar planets, including the space-based mission Kepler (1), are expected to detect hundreds of Jovian mass planets and tens of terrestrial mass planets. For many of these newly discovered planets, the intervals between successive transits will be measured with an accuracy of 0.1–100 minutes. We show that these timing measurements will allow for the detection of additional planets in the system (not necessarily transiting), via their gravitational interaction with the transiting planet. The transit time variations depend on the mass of the additional planet, and in some cases Earth-mass planets will produce a measurable effect.**

The one hundred or so currently known extrasolar planets (2) have revealed themselves through three types of phenomena: 1) short-duration brightness anomalies in gravitational microlensing events caused by planets near the lens star (3), 2) reflex motions of the central star (as revealed by radial velocity variations in the stellar spectrum or radio pulse arrival times) (4, 5, 6, 7), and 3) variations in the apparent stellar brightness caused by a planetary transit (passage of the planet in front of the star) (8, 9, 10, 11, 12). These approaches provide complementary information. Gravitational microlensing measurements primarily constrain the

ratio of planet mass to stellar mass. Microlensing surveys are sensitive to Earth-mass planets in principle but reveal little orbital information about the planets discovered. Radial velocity measurements allow for estimates of the orbital period, eccentricity, and minimum mass of the planet. With present technology, radial velocity surveys can only detect planets with masses greater than about 10 Earth masses (orbiting low mass stars) (13, 14, 15). Current transit observations allow for the determination of the orbital period and planetary radius. Transit surveys, particularly if space-based, will be sensitive to planets as small as Mercury’s for the smallest stars observed (1). Barring significant improvements in the precision of radial velocity measurements, the measurement of the mass and radius (and thus the density) of an Earth-sized extrasolar planet would appear to be out of reach.

Here we point out that variations in the time interval between transits, produced via gravitational interactions with additional planets, allow for the orbital period and mass of the additional planet to be determined from transit observations alone. In some instances, when two or more planets transit the same star, the density of the planets can be determined. This opens the possibility of obtaining considerably more information about transiting planets than has been previously thought.

The time interval between successive transits of an *unperturbed* planet is always the same, because the orbital period is constant. However, it has long been known that the presence of a third body can produce short-term variations, in addition to the more familiar long-term variations, of the period of a binary (16, 17). The same is true for planetary systems. It has been recently noted that the interval between successive transits of the extrasolar planet HD 209458b would vary by  $\pm 3$  s if a second planet (of mass  $10^{-4} M_{\odot}$ , period 80-day, and eccentricity  $e \sim 0.4$ ) existed in that system (18).

Over the course of their orbits the transiting planet and a second planet exchange energy and angular momentum as a result of their mutual gravitational interaction. This interaction, greatest at each planetary conjunction, results in short-term oscillations of the semimajor axes and eccentricities of the planets, which in turn alter the interval between successive transits. We first illustrate this effect by considering our solar system. Figure 1 shows the variation in the transit intervals of our terrestrial planets, recorded by distant observers located in the orbital plane of each planet. The gravitational perturbations among the planets in our solar system lead to transit interval variations ranging from tens of seconds, for Mercury, to thousands of seconds, for Mars. The variations for Earth and Venus show oscillations with the 583-day Earth-Venus synodic period.

Next we investigate the influence of an additional planet on the transit interval of HD 209458b. We integrate the heliocentric equations of motion of the hypothetical two-planet system (19) and test that the relative energy error of the system is less than  $10^{-12}$  to assure the reliability of our results. We assume that the two planets are coplanar, have orbits that are perpendicular to the sky plane, and have initially aligned orbital apsides. We include the mutual gravitational interactions of the planets and terms that account for the general relativistic (GR) influence of the central star (20) but neglect the terms for the GR influence of the planetary masses, terms for the oblateness of the star, as well as terms for the tidal interaction with the star. During the course

of each integration, we iteratively solve for the central transit times of the inner planet.

Figure 2 displays the interval between the times of successive transits of HD 209458b, with each panel showing the results for a different set of orbital parameters of a hypothetical exterior planet. The large spikes in the transit interval, evident in the top three panels of figure 2, occur near the times when the outer planet reaches its periastron. Hence, the orbital periods of both planets can be determined directly. We choose the period and eccentricity of the four hypothetical planets such that their pericenter distances are roughly the same. As a result, the largest transit interval variations have comparable magnitude. For clarity, we separate the light-time effect ( $2l$ ) (due to the varying distance between the star and the observer as the star moves with respect to the center of mass among the star and planets) from the dynamical effects described above.

Whether the presence of a given companion planet can be detected from short-term transit interval variations alone depends on the difference between the minimum and maximum transit interval. The black lines in figures 3 and 4 show those differences for Jupiter-mass ( $10^{-3} M_{\odot}$ ) and Earth-mass ( $3 \times 10^{-6} M_{\odot}$ ) perturbing planets, respectively, as a function of their orbital period (or semimajor axis) and eccentricity. In these calculations the star has mass  $M_* = M_{\odot}$ ; the transiting planet has the mass of Jupiter and an initial eccentricity and period of  $e_1 = 0.01$  and  $P_1 = 3.0$  d, respectively. For each perturber eccentricity, a range of perturber periods are tested, in increments of 0.1 d, starting with the minimum perturber periods that ensures that the orbits of the two planets do not initially cross. We follow the same numerical procedure described earlier. During each integration, simulating  $10^4$  d, we record the times of transit, from which the minimum and maximum intervals between transits were determined. As expected, for a given perturber eccentricity the period variation decreases as the perturber period and semimajor axis increase. Likewise, for a given perturber period, the variation is greater for larger perturber eccentricity. As indicated earlier, the transit interval variation is primarily a function of the periastron distance of the perturber. Comparison of the two figures confirms that the magnitude of the effect is proportional to the perturber mass. We also note that, for short time spans, the magnitude of the effect is independent of the mass of the transiting planet (a result that follows from the equivalence of inertial and gravitational mass).

Analytic estimates of the variation in transit intervals can be found by integration of Lagrange's equations of planetary motion (22). Given a transiting planet with semimajor axis  $a_1$  and period  $P_1$ , and a perturbing planet with semimajor axis  $a_2$  (assumed larger than  $a_1$ ), period  $P_2$ , and mass  $M_2$ , we find

$$\Delta t \sim \frac{45\pi}{16} \left( \frac{M_2}{M_*} \right) P_1 \alpha_e^3 \left( 1 - \sqrt{2} \alpha_e^{3/2} \right)^{-2} \quad (1)$$

where  $\alpha_e = \frac{a_1}{a_2(1-e_2)}$ . The red dashed lines in figures 3 and 4 show the estimate given by the expression above. Equation (1) was derived by assuming the perturber follows a parabolic orbit with a periastron distance of  $a_2(1 - e_2)$ . It significantly underestimates the actual variation in transit period for small period ratios and is best suited for  $e_2 \geq 0.3$ . The transit interval variations increase with  $P_1$  when the period ratio of the two planets is held fixed. Thus, the

detection of companions is easier for systems where the transiting planet is farther from the star. The timing variations are also larger for planets orbiting less massive stars, for a given perturbing planet mass.

As suggested by figure 2, the eccentricity of the outer planet can be estimated from the relative magnitudes of the variations  $\Delta t_{max}/\Delta t_{min}$ . If the period of the perturbing planet is much greater than that of the transiting planet, the final factor of equation (1) can be ignored. The resulting equation can be rearranged to provide an estimate of the mass of the perturbing planet

$$M_2 = \frac{16}{45\pi} M_* \frac{\Delta t_{max}}{P_1} \left( \frac{P_2}{P_1} \right)^2 (1 - e_2)^3, \quad (2)$$

given an estimate of  $e_2$ .

Large excursions in transit interval variation in figures 3 and 4 occur near small integer ratios of the orbital periods of the two planets. These correspond to mean-motion resonances, near which the planets undergo larger oscillations of semimajor axis and eccentricity (22). The width in semimajor axis of each resonance region is proportion to  $a_2 (M_*/M_2)^{1/2}$  and grows rapidly with increasing eccentricity (22). The ranges of perturber periods in figures 3 and 4 in which the transit interval variations appear irregular correspond to dynamical chaos resulting from the overlap of adjacent mean-motion resonances (23). We have excluded the ranges of perturber period in which this chaos results in short-term dynamical instability (since such planetary configurations are unlikely to be found).

The two planets of the GJ 876 system provide an excellent example of a 2:1 mean-motion resonance in an extrasolar planetary system. Due to the resonant gravitational interaction between the two planets, the orbital periods of the inner and outer planet vary from 30.1 d to 31.1 d and 60.0 d to 59.1 d, respectively, over a libration period of 550 d (24). Although careful photometric monitoring has excluded the possibility of transits of the inner planet of the GJ 876 system (25), such transit interval variations would be clearly seen if the inner planet transited.

In some cases, the libration period of a resonant system can be too long for the transit interval variations due to the resonance to be easily observed, even if the amplitude of the variation is large. GJ 876's short libration period,  $P_{lib}$ , results from the combination of its low-mass star ( $M_* = 0.4 M_\odot$ ) and massive planets ( $M_1 = 2 M_{jup}$ ,  $M_2 = 4 M_{jup}$ ), since  $P_{lib} \propto P_1 (M_*/M_2)^{1/2}$  (24, 22) (and depends upon the order of the resonance). Note that the  $10^4$  d integrations used for figures (3) and (4) are long enough to sample a full libration period for the low-order resonances. A corresponding system with a solar-mass star, a 1-year orbital period for the inner planet, and jupiter-mass planets in the 2:1 resonance would have a libration period of roughly 50 years. For earth-mass planets the libration period would be nearly 1000 years. These long-term effects would not be observable. However, the smaller transit interval variations that occur on the time scale of the orbital periods of the two planets, that are superimposed on longer period variations, could be observed.

The feasibility of this technique to detect additional planets in transiting systems depends on the physical and orbital properties of the multiple planet systems, as well as the accuracy with which the times of transit can be measured. Our expectations for systems with multiple

Neptune-mass to Jupiter-mass planets are guided by recent discoveries, as well as by the giant planets in our solar system. Fourteen (of 117) systems are known to have two or more planets. These have period ratios ranging from 2 to 150, and three are known or thought to be in mean motion resonances. In the solar system, neighboring giant planets have period ratios of two to three. The eccentricities of the planets in the solar system are small, but in many of the extrasolar planetary systems the eccentricities are substantial, ranging up to  $e = 0.7$ .

Both the theory of terrestrial planet formation and available observations suggest that the typical terrestrial planet system will have a configuration that results in variations in the transit interval of hundreds of seconds. Because the escape velocity from the surface of a terrestrial planet is smaller than the escape velocity from a solar mass star at roughly one AU, all the solid material in the region from a few tenths to one or two AU must either accrete into planets or fall onto the star. The resulting planets are as closely spaced as dynamical stability permits (26, 27). As observed in our solar system and in the pulsar planet system, the period ratios are of order two.

Assuming the observations during the ingress and egress of a transit are well-sampled, the error  $\sigma_{t_c}$  (due to photon statistics alone) associated with the measured time of the center of a transit of duration  $t_T$  is given by

$$\frac{\sigma_{t_c}}{t_T} \sim (\Gamma t_T)^{-1/2} \rho^{-3/2}, \quad (3)$$

where  $\Gamma$  is the photon count rate of the star and  $\rho = R_p/R_*$  is the ratio of the planet radius to the stellar radius. Kepler (*I*), a NASA Discovery mission, will monitor 100,000 A-M dwarf stars brighter than apparent magnitude  $V = 14$ , looking for transits of detecting Earth-sized planets in the “habitable zone” (28). For Kepler, with its 0.95 m diameter aperture,  $\Gamma = 7.8 \times 10^8 10^{-0.4(V-14)} \text{ hr}^{-1}$ , for a star of apparent magnitude  $V$ . For a Jupiter-sized planet in a 1-year orbit about a solar-mass star with  $V = 14$ , we find  $\sigma_{t_c} \sim 20 \text{ s}$  ( $\rho \sim 0.1$ ,  $t_T \sim 13\text{hr}$ ). For an Earth-sized planet,  $\sigma_{t_c} \sim 500 \text{ s}$  ( $\rho \sim 0.01$ ). These accuracies suggest that the transit period variations due to the gravitational influence of Earth-mass planets with small period ratios can be detected by Kepler. For brighter stars observed with large-aperture ground-based telescopes, the presence of more distant additional planets can be detected. For example, observing a  $V = 9$  star with a 6.5 m aperture telescope,  $\sigma_{t_c} \sim 0.2 \text{ s}$ .

One would like to measure the density of a transiting planet to determine if it is a rocky terrestrial planet such as the Earth, an ice/water giant such as Neptune, or a gas giant planet such as Jupiter. However, when a transiting planet is perturbed by another planet that does not transit, photometry yields an estimate of the radius of the transiting planet but not its mass, and the transit timings yield an estimate of the mass of the perturbing planet but not its radius. In the cases in which both planets transit their star the masses and radii of both planets can be estimated, allowing density determinations. This means that for some subset of the discovered planets (double transit systems), radial velocity observations will not be necessary to determine their masses and densities. This has important implications for the search for habitable planets.

If transits of one planet are seen, what is the probability of seeing transits of a second planet? Assuming such a planet exists and that the orbits of the two planets are coplanar, the probability

that the second planet also transits is simply  $a_1/a_2$  if  $a_2 > a_1$  (if  $a_2 < a_1$  transits of the second planet are assured in the case of coplanar orbits). If the orbits of the two planets are mutually inclined and one planet transits the center of the star, the probability that the second planet also transits is

$$P_{t_2} = \frac{2}{\pi} \arcsin \left( \frac{R_*}{a_2 \sin i'} \right), \quad (4)$$

where  $i'$  is the mutual inclination between the orbits of the two planets rather than the sky plane inclination. This assumes  $\sin i' > R_*/a_2$ , otherwise transits of the second planet are certain. For a solar-radius star, a mutual inclination of a few degrees, and a semimajor axis  $a_2 \sim 1$  AU, the probability is roughly 10%. Thus, such double transiting systems are likely to be found.

The Kepler team plans to search for transits with a consistent period, depth, and duration ( $I$ ). We caution that any detection algorithm that looks for evidence of periodic transits in the photometry must allow for variations in the transit period due to the perturbations from unseen planets. An overly restrictive test for periodicity might reject some of the most interesting and informative planetary systems. The GJ876 system discussed above, an extreme case, could easily be rejected as only quasiperiodic.

We also caution that experiments looking for gradual transit period variations due to slow secular trends must allow for the possibility of significant short-term variations in the transit period. Transit period variations due to orbital precession induced by the general relativistic effects of the central star, the oblateness of the star, or the presence of a distant additional planet (29) or due to the decay of the transiting planet's orbital semimajor axis as a result of dissipative tidal interaction between the star and planet (30), require many years to elapse before they can be detected; without careful monitoring in the interim to determine the short-term variations, the results of such experiments could be easily misinterpreted.

## References and Notes

1. W. J. Borucki, *et al.*, *Future EUV/UV and Visible Space Astrophysics Missions and Instrumentation*. Edited by J. Chris Blades, Oswald H. W. Siegmund. *Proceedings of the SPIE, Volume 4854*, pp. 129-140 (2003). (2003), pp. 129–140.
2. J. Schneider (2004). <http://www.obspm.fr/encycl/catalog.html>.
3. I. A. Bond, *et al.*, *ApJ* **606**, L155 (2004).
4. A. Wolszczan, D. A. Frail, *Nature* **355**, 145 (1992).
5. D. C. Backer, R. S. Foster, S. Sallmen, *Nature* **365**, 817 (1993).
6. M. Mayor, D. Queloz, *Nature* **378**, 355 (1995).
7. G. W. Marcy, R. P. Butler, *ApJ* **464**, L147+ (1996).

8. D. Charbonneau, T. M. Brown, D. W. Latham, M. Mayor, *ApJ* **529**, L45 (2000).
9. G. W. Henry, G. W. Marcy, R. P. Butler, S. S. Vogt, *ApJ* **529**, L41 (2000).
10. A. Udalski, *et al.*, *Acta Astronomica* **52**, 1 (2002).
11. A. Udalski, *et al.*, *Acta Astronomica* **52**, 115 (2002).
12. A. Udalski, *et al.*, *Acta Astronomica* **53**, 133 (2003).
13. B. E. McArthur, *et al.*, *ApJ* **614**, L81 (2004).
14. P. Butler, *et al.*, *ArXiv Astrophysics e-prints* (2004).
15. R. Narayan, A. Cumming, D. N. C. Lin, *ArXiv Astrophysics e-prints* (2004).
16. E. W. Brown, *MNRAS* **97**, 62 (1936).
17. S. Soderhjelm, *Astron. Astroph.* **42**, 229 (1975).
18. P. Bodenheimer, G. Laughlin, D. N. C. Lin, *ApJ* **592**, 555 (2003).
19. J. Stoer, R. Bulirsch, *Introduction to Numerical Analysis* (New York: Springer-Verlag, 1980).
20. T. R. Quinn, S. Tremaine, M. Duncan, *AJ* **101**, 2287 (1991).
21. R. W. Hilditch, *An Introduction to Close Binary Stars* (An Introduction to Close Binary Stars, by R.W. Hilditch. Cambridge University Press, 2001, 392 pp., 2001).
22. C. D. Murray, S. F. Dermott, *Solar System Dynamics* (Cambridge: University Press, —c1999, 1999).
23. J. Wisdom, *AJ* **85**, 1122 (1980).
24. G. Laughlin, J. E. Chambers, *ApJ* **551**, L109 (2001).
25. G. Laughlin (2004). <http://www.transitsearch.org>.
26. J. E. Chambers, G. W. Wetherill, *Icarus* **136**, 304 (1998).
27. E. Kokubo, S. Ida, *Icarus* **131**, 171 (1998).
28. J. F. Kasting, D. P. Whitmire, R. T. Reynolds, *Icarus* **101**, 108 (1993).
29. J. Miralda-Escudé, *ApJ* **564**, 1019 (2002).
30. D. D. Sasselov, *ApJ* **596**, 1327 (2003).

31. This work was supported in part by the National Science Foundation under Grant No. PHY99-07949 and by NASA grant NAG5-9678. This research was supported by NSERC of Canada, and by the Canada Research Chair program. We are grateful to the Kavli Institute for Theoretical Physics, where much of this investigation was carried out. We thank Scott Gaudi and Joshua Winn for helpful discussions and careful reviews of the manuscript.



**Fig. 1.** Transit times of the terrestrial planets: The variation of the interval between successive transits of terrestrial planets, induced by the other planets in the solar system. To guide the eye, the solid line connects the times of each transit.

**Fig. 2.** Transit times of HDf 209458b: The interval between successive transit centers of HD 209458b as a function of time, with each panel showing the results for a different set of orbital parameters for the hypothetical second planet.

**Fig. 3.** Variations induced by a Jupiter-mass planet: Variations in the interval between successive transits of a planet with  $P_1 = 3$  d,  $e_1 = 0.01$ ,  $M_1 = 10^{-3}M_\odot$ , induced by a second planet with mass  $M_2 = 10^{-3}M_\odot$ .

**Fig. 4.** Variations induced by an Earth-mass planet: Variations in the interval between successive transits of a planet with  $P_1 = 3$  d,  $e_1 = 0.01$ ,  $M_1 = 10^{-3}M_\odot$ , induced by a second planet with mass  $M_2 = 3 \times 10^{-6}M_\odot$ .

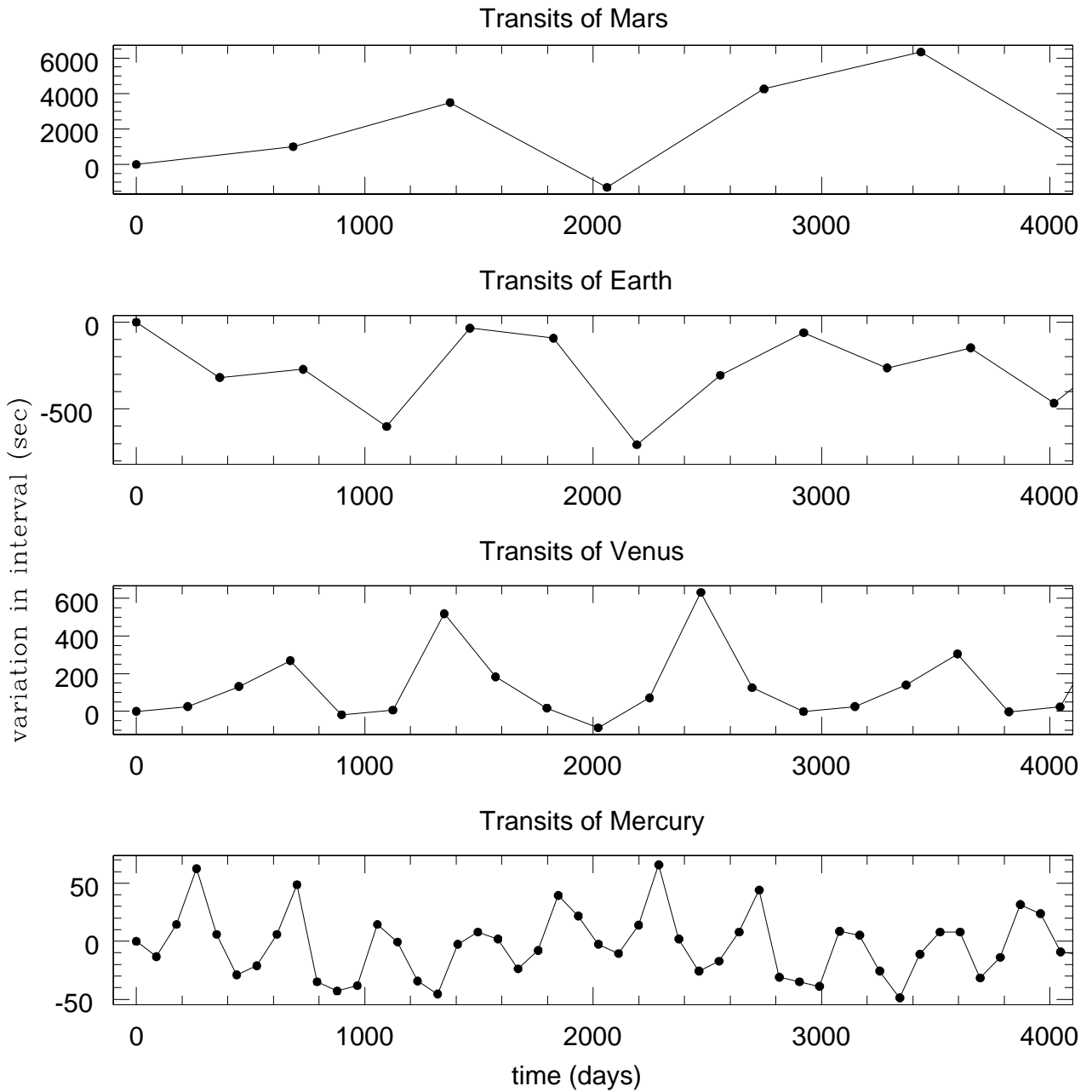


Figure 1: Variation of transit periods of the terrestrial planets, as would be recorded by distant observers located in the orbital plane of each planet.

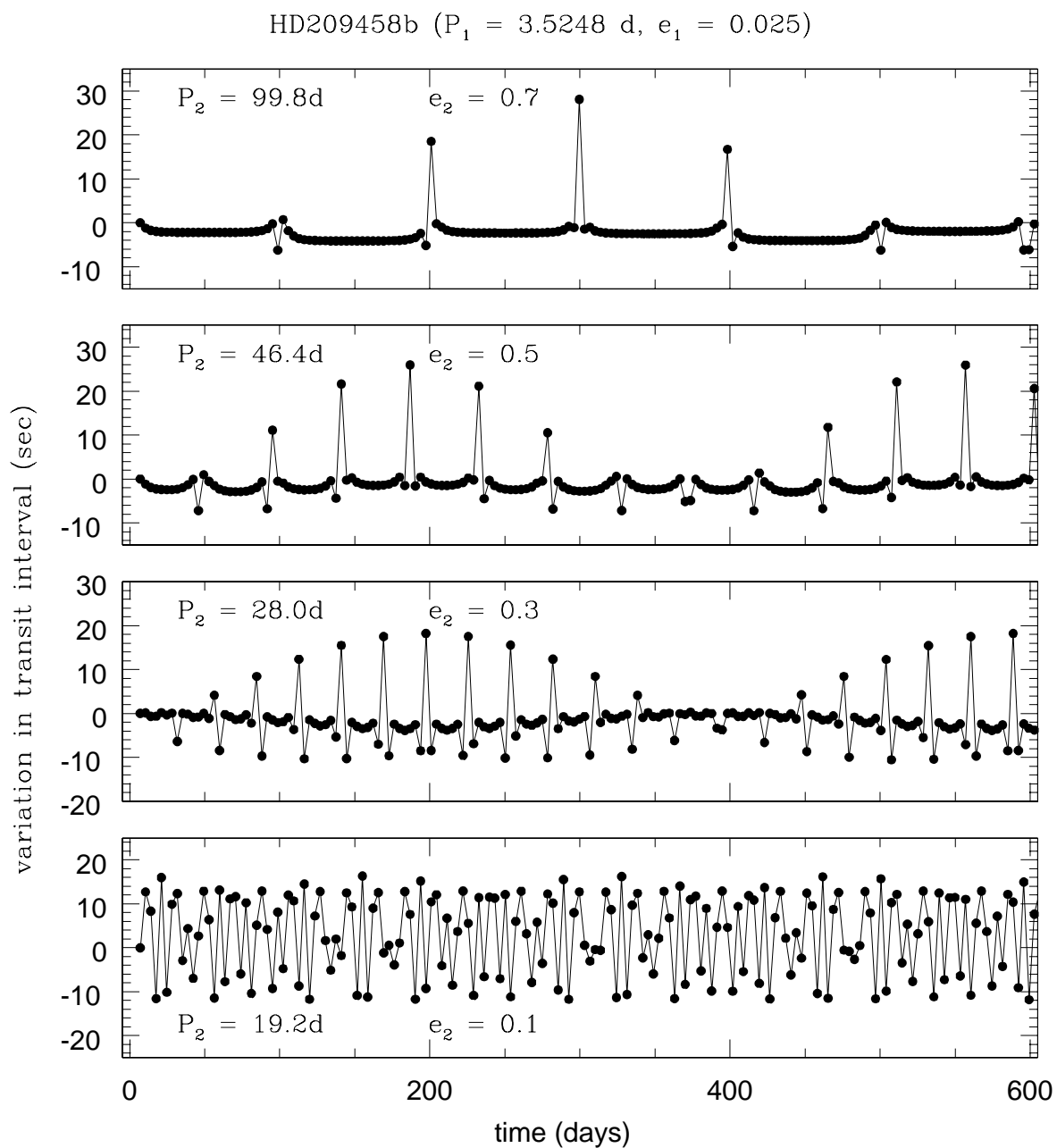


Figure 2: Variations of the transit period of HD 209458b, induced by a hypothetical second planet.

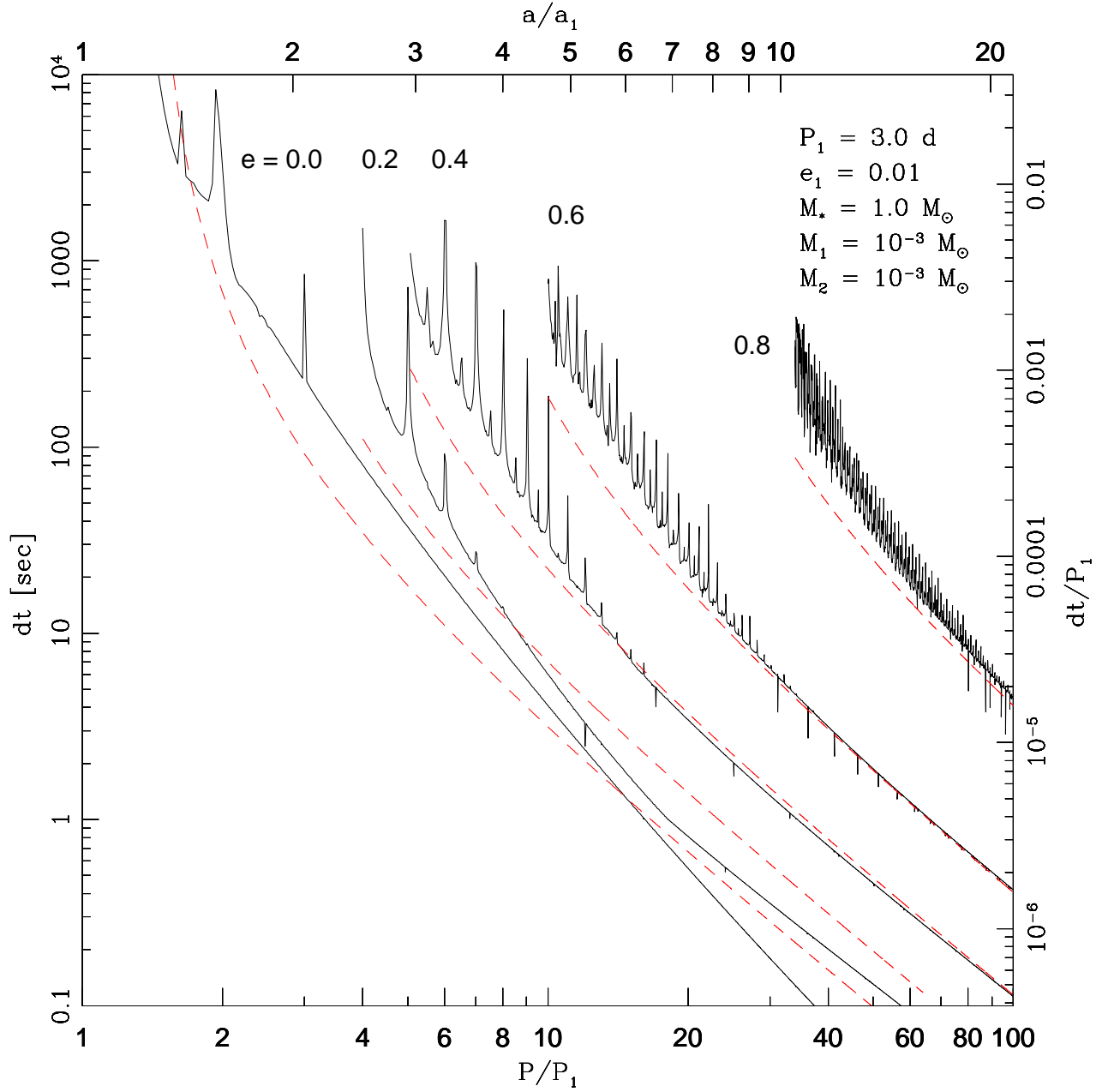


Figure 3: Variations in the interval between successive transits of a planet with  $P_1 = 3$  d,  $e_1 = 0.01$ ,  $M_1 = 10^{-3} M_\odot$  induced by a second planet with mass  $M_2 = 10^{-3} M_\odot$ .

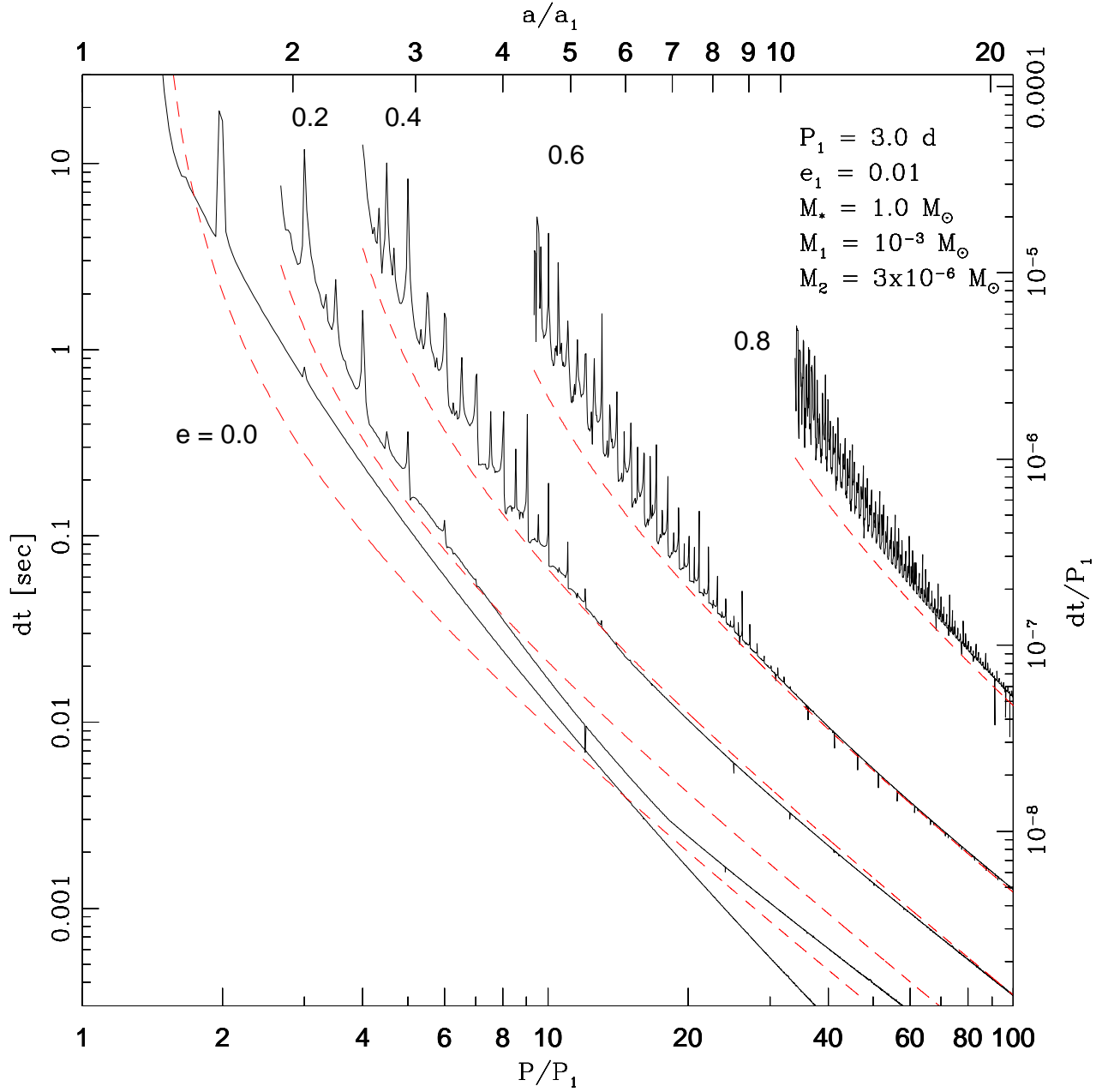


Figure 4: Variations in the interval between successive transits of a planet with  $P_1 = 3 \text{ d}$ ,  $e_1 = 0.01$ ,  $M_1 = 10^{-3} M_\odot$  induced by a second planet with mass  $M_2 = 3 \times 10^{-6} M_\odot$ .